PHILOSOPHICAL TRANSACTIONS OF THE ROYAL SOCIETY A MATHEMATICAL, PHYSICAL & ENGINEERING SCIENCES

The Magnetohydrodynamics of Energy Release in Solar Flares [and Discussion]

E. R. Priest, K. J. H. Phillips and M. G. Haines

Phil. Trans. R. Soc. Lond. A 1991 **336**, 363-380
doi: 10.1098/rsta.1991.0087

The magnetohydrodynamics of energy release in solar flares

By E. R. Priest

Department of Mathematical and Computational Sciences, The University, St Andrews KY16 9SS, U.K.

A large solar flare is thought to occur when a sheared magnetic arcade loses equilibrium or goes unstable and erupts, and drives magnetic reconnection in the stretched-out magnetic field lines. These two key processes of magnetic eruption and magnetic energy conversion by reconnection are reviewed briefly, with an account of recent analytical and numerical models. When the height or length of a prominence in a sheared coronal arcade is too great it may erupt and drive the formation and reconnection of a current sheet below it. Recent progress in fast steady-state reconnection theory has explained many puzzling features of numerical experiments, and has shown how a new process of magnetic flipping can reconnect fields in three dimensions. Also numerical modelling of the formation of flare loops and ribbons by reconnection has accounted for many observational properties.

1. Introduction

At the core of a solar flare magnetic energy is believed to be released by the process of magnetic reconnection. In this paper I shall describe, first, some recent developments in the basic theory of reconnection and, secondly, the way the process works in the flare context. Throughout, the stress will be on theoretical aspects of energy release, since the observational aspects are treated by Canfield *et al.* (1991) in the following paper.

The amount of magnetic energy contained in coronal structures is certainly sufficient for a flare. For example, an arcade of field strength 500 G, radius 20 Mm, length 100 Mm and shear angle 45° contains an excess energy of 6×10^{25} J (6×10^{32} erg), sufficient for a large flare, whereas a loop of field strength 500 G, radius 5 Mm, length 100 Mm and twist 2π contains an excess energy of 7×10^{23} J, sufficient for a small flare. Also, there is enough time to store the energy in excess of potential by slow photospheric motions, injecting the required Poynting flux. For example, footpoints moving at 1 km s^{-1} cover a distance of 100 Mm in a day.

However, the timescale for energy release due to magnetic diffusion (ohmic dissipation) over a length-scale l is

$$\tau_d = l^2/\eta,$$

where $\eta(=(\mu\sigma)^{-1})$ is the magnetic diffusivity and σ is the electrical conductivity; and, for a global length-scale $l\approx10$ Mm, this time is of order 10^{11} s, much too long for a flare. The result is that one needs to create extremely small structures with length-scales of 1 km or less in order to release the energy fast enough. The main questions we therefore need to answer from a magnetohydrodynamic (MHD) viewpoint are: how does the magnetic structure go unstable and how in detail is the energy released?

Phil. Trans. R. Soc. Lond. A (1991) **336**, 363–380
Printed in Great Britain

2. Basic theory of magnetic reconnection

Oppositely directed magnetic field lines in two dimensions may be carried towards one another by a flow, and broken and reconnected in a region of very strong magnetic gradient near an X-type neutral point. The physical effects of this process are wide-ranging: the global topology and magnetic connectivity may be changed, which affects the pathways for flow of fast particles and heat; stored magnetic energy is converted into heat and kinetic energy, so that hot fast streams of plasma are ejected from the reconnection site; large electric currents and fields, shock waves, filamentary structures and turbulence are created, all of which may help in accelerating fast particles.

The two basic equations of MHD (see, for example, Priest 1982) are the induction equation

$$\partial \boldsymbol{B}/\partial t = \nabla \times (\boldsymbol{v} \times \boldsymbol{B}) + \eta \nabla^2 \boldsymbol{B} \tag{2.1}$$

and the equation of motion

$$\rho \, \mathrm{d}\boldsymbol{v}/\mathrm{d}t = -\nabla p + \boldsymbol{j} \times \boldsymbol{B}, \tag{2.2}$$

which determine the magnetic field ($\boldsymbol{B}$) and plasma velocity ($\boldsymbol{v}$). According to (2.1), changes of $\boldsymbol{B}$ in time are produced partly by the advection of magnetic field lines with the plasma (the first term on the right) and partly by diffusion of the field lines (the second term on the right). Almost everywhere the first effect dominates and the magnetic field is frozen to the plasma. The exception is in very narrow regions of high magnetic gradient and large electric current

$$\boldsymbol{j} = (\nabla \times \boldsymbol{B})/\mu. \tag{2.3}$$

Here the magnetic field diffuses and energy is converted into heat ohmically (j^2/σ). The integral of (2.1) is Ohm's Law,

$$\boldsymbol{E} = -\boldsymbol{v} \times \boldsymbol{B} + \boldsymbol{j}/\sigma \tag{2.4}$$

$$= -\boldsymbol{v} \times \boldsymbol{B} + \eta \nabla \times \boldsymbol{B} \tag{2.5}$$

and in an ideal plasma, where diffusion is small, the second term on the right-hand side is negligible.

The equation of motion (2.2) describes how the plasma is accelerated by a plasma pressure gradient (∇p) and a magnetic force ($\boldsymbol{j} \times \boldsymbol{B}$), which may be decomposed by (2.3) into two terms, a magnetic pressure gradient ($-\nabla(B^2/2\mu)$) and a magnetic tension force ($(\boldsymbol{B}.\nabla)\boldsymbol{B}/\mu$). The ratio of the pressure gradient to the magnetic force is in order of magnitude the plasma beta,

$$\beta = 2\mu p/B^2. \tag{2.6}$$

Also, by equating the inertial term on the left of (2.2) with the magnetic force, we obtain in order of magnitude that the plasma is accelerated to a speed equal to the Alfven speed,

$$v_{\mathrm{A}} = B/(\mu\rho)^{\frac{1}{2}}. \tag{2.7}$$

Classical theory

The classical reconnection mechanisms are illustrated in figure 1. In constructing such mechanisms the main questions to answer were: what is the structure of the magnetic field and what is the fastest reconnection rate?

PHILOSOPHICAL TRANSACTIONS OF THE ROYAL SOCIETY A MATHEMATICAL, PHYSICAL & ENGINEERING SCIENCES

Figure 1

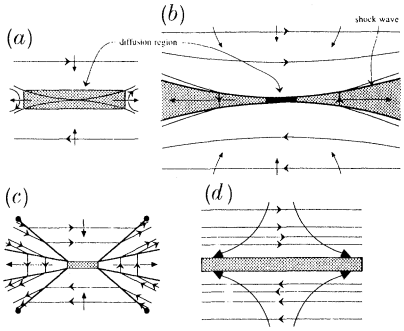

Figure 2

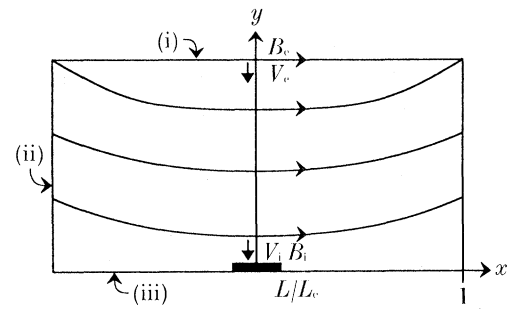

Figure 1. The classical energy conversion mechanisms of (*a*) Sweet–Parker, (*b*) Petschek, (*c*) Sonnerup and (*d*) Sonnerup & Priest.

Figure 2. Notation and boundary conditions for the unified theory (Priest & Forbes 1986). (i) $B_{1x} = 0$, (ii) $\partial B_{1y}/\partial x = 0$, (iii) $B_{1y} = f(x)$.

The Sweet (1958) model is a simple diffusion region or current sheet of length $2L$ and width $2l$ between oppositely directed magnetic fields. One may simply write down order-of-magnitude relations between the inflow speed ($v_{\rm i}$) and the outflow speed ($v_{\rm Ai}$), which is the Alfven speed based on the inflow magnetic field ($B_{\rm i}$). Thus for a steady state the plasma flows in at the speed

$$v_{\rm i} = \eta/l \tag{2.8}$$

at which the magnetic field is trying to diffuse outwards. Also the conservation of mass into and out of the region gives

$$Lv_{\rm i} = lv_{\rm Ai}. \tag{2.9}$$

Elimination of l between (2.8) and (2.9) gives in dimensionless form the inflow Alfven Mach number (i.e. the reconnection rate) as

$$M_{\rm i} = 1/R_{\rm mi}^{\frac{1}{2}}, \tag{2.10}$$

where $M = v/v_{\rm A}$ and $R_{\rm m} = Lv_{\rm A}/\eta$ is the magnetic Reynolds number. In practice $R_{\rm m}$ is typically 10^6–10^{12} and so the reconnection is very slow ($M_{\rm i} \sim 10^{-3}$–10^{-6}), which was why Petschek sought a faster mechanism to explain energy release in a flare.

In the Petschek mechanism (1964) the diffusion region occupies only a small central location, while most of the energy conversion occurs at standing slow-mode shock waves that accelerate and heat the plasma to form two hot fast outflowing streams. His analysis is disarmingly simple. The magnetic field decreases substantially from a uniform value ($B_{\rm e}$) at large distances to a value $B_{\rm i}$ at the entrance to the diffusion region, while the flow speed increases from $v_{\rm e}$ to $v_{\rm i}$. The aim is to determine for a given $B_{\rm e}$ the maximum value of $v_{\rm e}$ (in dimensionless form $M_{\rm e} = v_{\rm e}/v_{\rm Ae}$). The effect of the shocks is to provide a normal field component $B_{\rm N}$, which essentially produces the distortion in the inflow field from the uniform value $B_{\rm e}$ at large distances. Thus if the inflow field is potential, the distortion may be regarded as being produced by a series of monopole sources along the x axis between $|x| = L$ and $|x| = L_{\rm e}$, say. The result is that, as the diffusion region is approached the field strength falls to

$$B_{\rm i} = B_{\rm e} - (4B_{\rm N}/\pi) \ln (L_{\rm e}/L). \tag{2.11}$$

At the shock waves the condition that they be standing is $B_N/\sqrt{(\mu\rho)} = v_e$ and Petschek estimates the maximum reconnection rate (M_e^*) by putting $B_i = \frac{1}{2}B_e$ in (2.11) to be

$$M_e^* = \pi/8 \ln R_{me}. \tag{2.12}$$

In practice this is typically 0.01, which is much greater than the Sweet–Parker rate.

In Sonnerup's (1970) model an extra set of discontinuities is standing in the flow ahead of the slow shocks, but Vasyliunas (1975) pointed out that these are slow-mode expansion waves: they need to be generated externally at discrete points in the flow which would not be present in astrophysical applications. Sonnerup & Priest (1975) discovered an exact solution of the nonlinear MHD equations in which an incompressible stagnation-point flow carries in oppositely directed (but straight) magnetic field lines. Their model has since been generalized by Gratton *et al.* (1988) and Jardine *et al.* (1991) to include more general viscous flows.

3. Unified theory of fast, steady, almost-uniform reconnection

Vasyliunas (1975) clarified the physics of Petschek's mechanism by pointing out that the inflow region has the character of a *fast-mode expansion* with the pressure and field strength decreasing and the flow converging as the magnetic field is carried in. A *fast-mode disturbance* has the plasma and magnetic pressure increasing or decreasing together, while a *slow-mode disturbance* has the plasma pressure changing in the opposite sense to the magnetic pressure. An *expansion* makes the pressure decrease while a *compression* makes it increase, even in the incompressible limit. Sonnerup's model possesses slow-mode expansions that are unlikely to be found in astrophysics because they are discrete. Vasyliunas suggested that a Sonnerup-like solution may, however, be possible with a diffuse slow-mode expansion spread throughout the inflow region, making the field strength increase, the pressure decrease and the flow diverge as the field lines are carried in, although he was unable to find such a solution.

I wanted to understand Vasyliunas's distinction mathematically and was also puzzled at many strange features of some of the numerical reconnection experiments, such as much longer diffusion regions than Petschek, diverging flows and large pressure gradients. Also, can a Sonnerup-like solution be found without the extra discontinuities? And can a model in a finite region be produced, like the numerical experiments?

Terry Forbes and I (Priest & Forbes 1986) tried to answer such questions by seeking fast, steady, almost-uniform reconnection solutions to the equations for two-dimensional, incompressible flow, namely

$$\rho(\boldsymbol{v}.\nabla)\boldsymbol{v} = -\nabla p + (\nabla \times \boldsymbol{B}) \times \boldsymbol{B}/\mu, \tag{3.1}$$

$$\boldsymbol{E} + \boldsymbol{v} \times \boldsymbol{B} = \boldsymbol{0}, \tag{3.2}$$

$$\nabla.\boldsymbol{v} = \nabla.\boldsymbol{B} = 0. \tag{3.3}$$

The solutions are *almost uniform* in the same sense as Petschek's, namely that one performs a linear expansion about a uniform field

$$\boldsymbol{B} = B_0\hat{\boldsymbol{x}} + \boldsymbol{B}_1 + \ldots, \quad \boldsymbol{v} = \boldsymbol{v}_1 + \ldots.$$

PHILOSOPHICAL TRANSACTIONS OF THE ROYAL SOCIETY A MATHEMATICAL, PHYSICAL & ENGINEERING SCIENCES

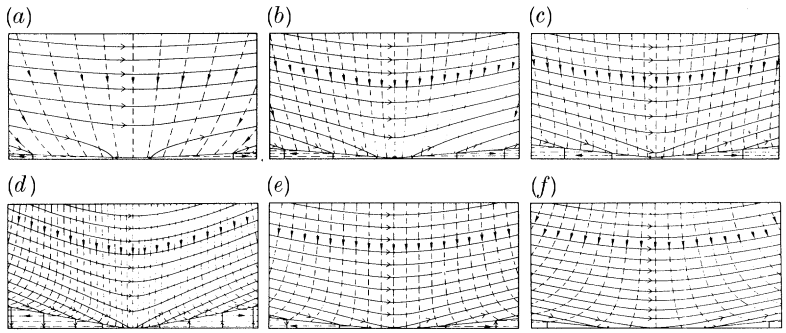

Figure 3. Magnetic field lines and streamlines for several members of the unified theory (Priest & Forbes 1986). (*a*) Slow compression ($b_0 < 0$), (*b*) Petschek ($b_0 = 0$), (*c*) hybrid expansion ($0 < b_0 < 2/\pi$), (*d*) hybrid expansion ($2/\pi < b_0 < 1$), (*e*) Sonnerup-like ($b_0 = 1$), (*f*) flux pile-up ($b_0 > 1$).

Equation (3.1) then reduces to the equation for a magnetostatic field

$$\nabla^2 A_1 = -(\mu/B_0)\,\mathrm{d}p_1/\mathrm{d}y, \tag{3.4}$$

where $$B_{1x} = \partial A_1/\partial y, \quad B_{1y} = -\partial A_1/\partial x.$$

The solution to (3.4) subject to the boundary conditions (figure 2) that

$$B_{1x} = 0 \quad \text{on } y = L, \quad \partial B_{1y}/\partial x = 0 \quad \text{on } x = L, \quad B_{1y} = 0 \quad \text{on } x = 0$$

$$B_{1y} = f(x) = \begin{cases} 2B_{\mathrm{N}}\, x/L, & 0 \leqslant x \leqslant L, \\ 2B_{\mathrm{N}}, & L \leqslant x \leqslant L_{\mathrm{e}}, \end{cases}$$

is $$A_1 = -\sum_0^\infty \frac{a_n}{(n+\frac{1}{2})\,\pi}\left(by - \cos\left[(n+\tfrac{1}{2})\,\pi\,\frac{x}{L}\right]\cosh\left[(n+\tfrac{1}{2})\,\pi\left(1-\frac{y}{L}\right)\right]\right), \tag{3.5}$$

where $$a_n = \frac{4B_N \sin\left[(n+\frac{1}{2})\,\pi L/L_{\mathrm{e}}\right]}{L/L_{\mathrm{e}}(n+\frac{1}{2})^2\pi^2 \cosh\left[(n+\frac{1}{2})\,\pi\right]}.$$

The solutions depend on a parameter b. When $b = 0$ this represents a Petschek-type solution with a weak fast-mode expansion. From (3.2) the first-order flow ($\boldsymbol{v}_1 = (E/B_0)\hat{\boldsymbol{y}}$), is uniform but the second-order flow is converging. By calculating B_{i} one can deduce a relation between M_{e} and M_{i}, which shows that, as Petschek had expected, M_{e} does indeed possess a maximum value which is close to Petschek's estimate.

When $b = 1$, the inflow field on the y-axis is uniform, and so we have found the Sonnerup-like solution with a slow-mode expansion across the whole inflow region. However, there are many other solutions for the other values of the parameter b, which is determined by the nature of the flow on the inflow boundary, since the horizontal flow speed at the corner $(x, y) = (L_{\mathrm{e}}, L_{\mathrm{e}})$ is proportional to $(b - 2/\pi)$. As b increases, so the inflow turns from being converging (and therefore producing slow-mode compressions) to being diverging (with strong slow-mode expansions). The latter comprise a *flux pile-up régime* with long diffusion regions. The resulting reconnection rate (M_{e}) is found to be faster than the Petschek rate for régimes with $b > 0$.

The main results from the above analysis are that the type of reconnection régime and the rate of reconnection depend sensitively on the inflow boundary conditions,

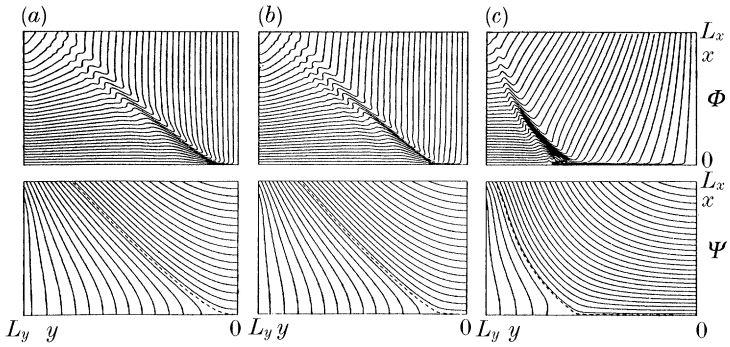

Figure 4. Numerical experiment on reconnection (Biskamp 1986).

with the Petschek ($b = 0$) and Sonnerup-like ($b = 1$) solutions being particular members of a much wider class. Jardine & Priest (1988) have recently extended the theory to include higher orders, compressibility and energetics. Also, it has been compared with a variety of numerical experiments (Forbes & Priest 1987).

4. Non-uniform reconnection with separatrix jets

Numerical experiments such as that shown in figure 4 reveal four puzzling features that are not present in the classical models of reconnection: (i) different types of inflow; (ii) separatrix jets; (iii) reversed current spikes; (iv) highly curved field lines in the inflow region.

The first feature is one which Priest & Forbes (1986) attempted to model with their unified almost-uniform theory. The other three features have been tackled in a new non-uniform theory by Priest & Lee (1990).

Feature (iii), the reversed current spikes at the ends of the diffusion region, slows down the streams of plasma that are emerging from the diffusion region and partly diverts them along the separatrix jets. This is partly a consequence of imposing boundary conditions at the outflow boundary that give a mismatch with the outflow from the diffusion region.

By contrast, feature (iv), the highly curved inflow field lines and the associated wide shock angle, is a direct result of the form of the inflow boundary conditions. In general the number of such conditions that can be imposed equals the number of MHD characteristics that are propagating information into the region. For our case of two-dimensional, sub-Alvenic, incompressible, essentially ideal flow, there are three imposed conditions. For instance, if one prescribes

$$v_x = 0, \quad v_y = \text{const.}, \quad p = \text{const.} \tag{4.1}$$

on the inflow boundary (AD), a solution of the MHD equations (3.1)–(3.3) is

$$B_x = \text{const.}, \quad B_y = 0,$$

so that the straight field lines are carried in by a uniform flow without curving and reconnection is impossible. If, on the other hand, boundary conditions only slightly different from (4.1) are imposed, reconnection with weakly curved inflow field lines may be produced, as in the Priest–Forbes theory. Thus it is entirely reasonable to expect that conditions greatly different from (4.1) could produce a highly curved inflow.

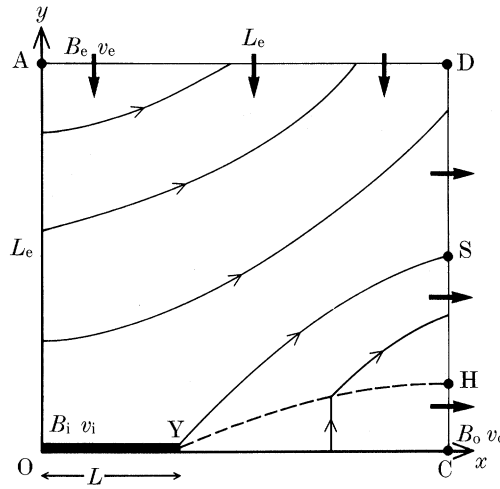

Figure 5. The notation for reconnection with a highly curved inflow (Priest & Lee 1990).

Now equation (3.3) may be satisfied identically by writing $\boldsymbol{v}$ and $\boldsymbol{B}$ in terms of a stream function (Ψ) and flux function (A), namely

$$v_x = \partial\Psi/\partial y, \quad v_y = -\partial\Psi/\partial x, \quad B_x = \partial A/\partial y, \quad B_y = -\partial A/\partial x.$$

Then one may tackle in three steps the problem of nonuniform reconnection with an imposed inflow (v_e) and field strength (B_e) on the inflow boundary producing a diffusion region (OY) of half-length L with a separatrix YS and slow shock YH (figure 5).

First of all, in the upstream region ahead of YH suppose for simplicity that both the plasma speed (v) and sound speed are much smaller than the Alfven speed (v_A). Then (3.1) implies that $j = 0$, and so for a potential field with a current sheet we may use complex variable theory to pick

$$B_y + \mathrm{i}B_x = B_i(z^2/L^2 - 1)^{\frac{1}{2}}, \tag{4.2}$$

where $z = x + \mathrm{i}y$ and there is a cut in the complex plane (a current sheet) from $z = -L$ to $z = L$. Then (3.2) implies that the flow velocity may be deduced from

$$\Psi = v_e B_e \int \frac{\mathrm{d}s}{B}, \tag{4.3}$$

where the integral is along a field line. The second step is to calculate the position of the shock from the characteristic curve

$$\Psi + A = \text{const.}$$

that passes through the end point (Y) of the diffusion region. Then the shock relations are applied to deduce the conditions just downstream of YH. Finally, one needs to solve the MHD equations in the downstream region subject to the appropriate boundary conditions at the shock and at the outflow boundary CH. In general these equations may be written

$$\boldsymbol{v}.\nabla A = -v_e B_e, \tag{4.4}$$

$$\boldsymbol{v}.\nabla\omega = \boldsymbol{B}.\nabla j, \tag{4.5}$$

where $\omega = -\nabla^2\Psi$ is the vorticity.

Figure 6

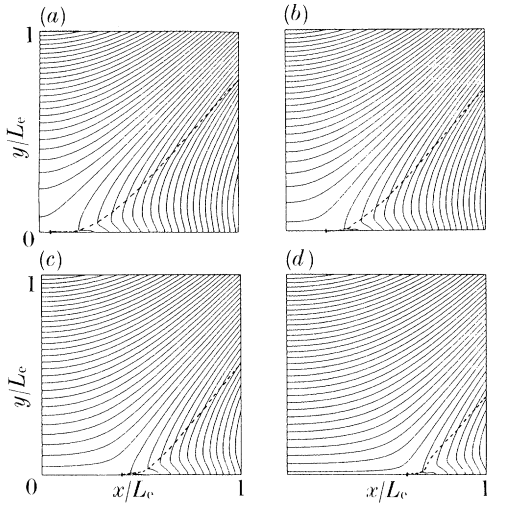

Figure 7

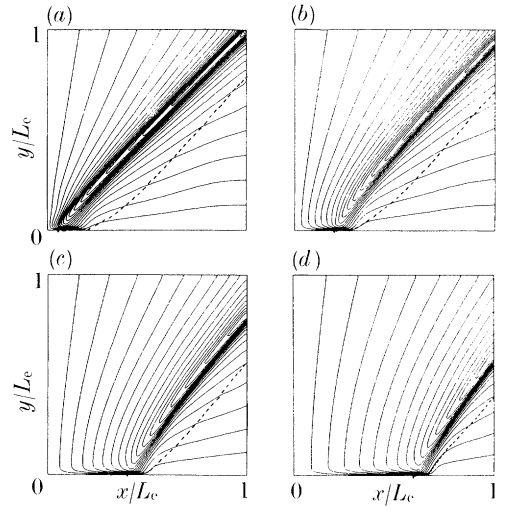

Figure 6. Field lines for one quadrant of non-uniform reconnection (Priest & Lee 1990). $L = 0.05\ L_e$ (*a*), $0.2\ L_e$ (*b*), $0.4\ L_e$ (*c*), $0.6\ L_e$ (*d*).

Figure 7. Streamlines corresponding to figure 6.

For example, the results of assuming $v \gg v_A$ and so taking $\omega = 0$ or

$$\nabla^2 \Psi = 0,$$

with Ψ imposed along the boundary YHC and $\Psi =$ const. on YC are shown in figures 6 and 7. The shock (strictly speaking an Alfvenic discontinuity of slow-mode compressional type in this incompressible model) is shown dashed but is rather weak and has little effect on the magnetic field. The effect of the reversed current spike downstream of the diffusion region shows up in the field lines of abnormal curvature and in the spreading of the streamlines. Also the separatrix jet is prominent and makes streamlines follow the separatrix as they pass through it. As the current sheet decreases in length, so the inflow speed increases up to a value that depends on the inflow Alfven Mach number. Results have also been obtained by solving the full equations (4.4) and (4.5).

5. Three-dimensional reconnection

In two dimensions, reconnection is now fairly well understood. In the ideal region around an X-type neutral point we have in cartesian coordinates

$$E_z + v_x B_y - v_y B_x = 0, \tag{5.1}$$

where for a steady-state process $\nabla \times \boldsymbol{E} = \boldsymbol{0}$ implies that E_z is constant. Thus reconnection can only take place at X-type neutral points and, as such a point is approached, the speed $v_\perp$ perpendicular to the field lines approaches infinity.

In three dimensions our understanding is very hazy and has been reviewed by Sonnerup (1988). Even our definition of reconnection is a matter for debate (Hesse & Schindler 1988; Schindler *et al.* 1988). The most intuitive way is in terms of a change of field-line connectivity, but a new definition has recently been proposed by Priest & Forbes (1989), who suggest that it occurs when there is a *singular line*, which

PHILOSOPHICAL TRANSACTIONS OF THE ROYAL SOCIETY A MATHEMATICAL, PHYSICAL & ENGINEERING SCIENCES

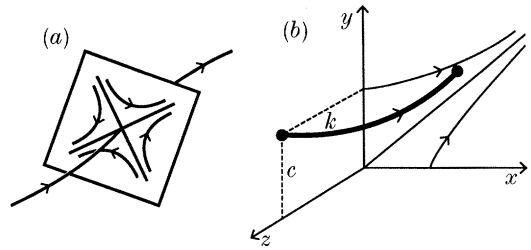

Figure 8. (*a*) Characteristic coordinates for the field $\boldsymbol{B} = (y, x, -1)$, (*b*) reconnection at the field line with $k = k_0$, $c = c_0$.

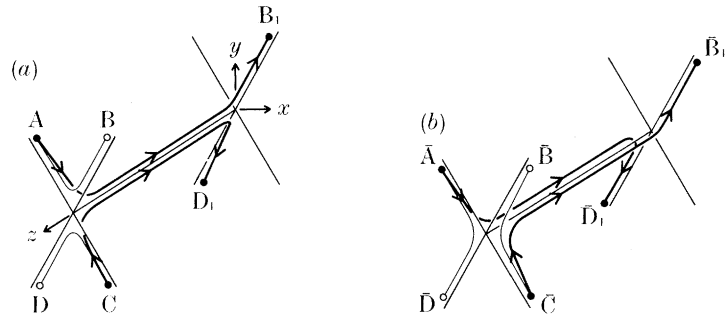

Figure 9. The mapping of magnetic field lines from one plane ($z = L$) to another ($z = 0$), showing several field lines. As one footpoint moves from A (*a*) to $\bar{\text{A}}$ (*b*), the opposite end flips rapidly from B_1 to $\bar{\text{D}}_1$ (Priest & Forbes 1991).

is defined to be a field line with two properties: first, it has a nearby X-type topology in the sense that field lines in a plane perpendicular to the field line are hyperbolic; secondly, it has an electric field along it. In general, a sheared magnetic configuration may possess a whole continuum of potential singular lines, and which one supports reconnection depends on the imposed flow velocity or electric field.

For example, Priest & Forbes (1989) are able to show what flow or electric field produces kinematic reconnection along any field line of the field

$$(B_x, B_y, B_z) = (y, x, -1), \tag{5.2}$$

which consists of the usual X-type field in the xy plane together with a uniform field in the z direction (figure 8).

Previously, it had been thought (see, for example, Lau & Finn 1990) that reconnection can only take place in three dimensions at a null-point, where all three components of the magnetic field vanish. Priest & Forbes (1991), however, have demonstrated that reconnection can take place in any sheared field, by a new process called *magnetic flipping*. Consider a sheared field such as (5.2) joining one plane to another (figure 9). Suppose there is a two-dimensional stagnation-point flow with streamlines in planes parallel to the xy plane. Assume that the magnetic footpoints A and C in one plane are frozen to the flow and ask what happens in the other plane ($z = 0$). Although the plasma moves slowly from B_1 to $\bar{\text{B}}_1$ and D_1 to $\bar{\text{D}}_1$, the magnetic footpoint B_1 rapidly flips down from B_1 to $\bar{\text{D}}_1$, and D_1 flips rapidly up to $\bar{\text{B}}_1$. In other words, the magnetic field reconnects. However, this process is very different from two-dimensional reconnection, where the ideal equations fail in small regions around the X-point, since now diffusion takes place everywhere along the surface BD (and/or AC).

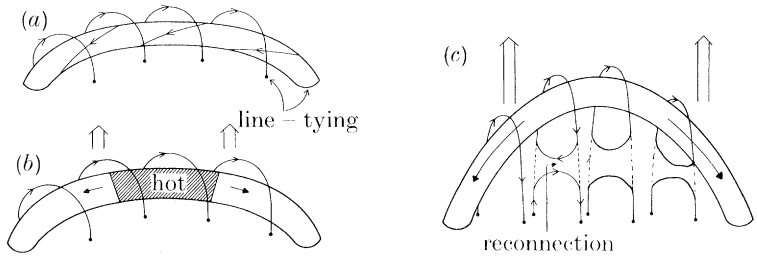

Figure 10. The overall scenario for a large (two-ribbon) flare. (*a*) Equilibrium, (*b*) slow rise, (*c*) fast eruption upwards.

Mathematically, one seeks steady-state solutions for the flow and electric field to the equations

$$\nabla \times \boldsymbol{E} = \boldsymbol{0} \tag{5.3}$$

and

$$\boldsymbol{E} + \boldsymbol{v} \times \boldsymbol{B} = \boldsymbol{0} \tag{5.4}$$

in the ideal region for the magnetic field (5.2). The solutions are of the form

$$E_x = \frac{E_z y}{y^2 - x^2} + xF(y^2 - x^2), \quad E_y = -\frac{E_z x}{y^2 - x^2} - yF(y^2 - x^2), \tag{5.5}$$

$$v_x = \frac{y v_y - E_z}{x}, \quad v_z = -\frac{v_y}{x} + \frac{E_z y/x}{y^2 - x^2} + F(y^2 - x^2), \tag{5.6}$$

and so possess singular jetting at the surfaces $y = \pm x$. The singularities may be resolved as boundary layers by resistive and viscous effects.

6. Reconnection in solar flares

Magnetic reconnection has several roles in flares. It may create small flares when newly emerging flux or laterally moving flux interacts with neighbouring flux of opposite polarity (Priest 1987). This process of emergence has been modelled numerically by Forbes & Priest (1984), and many aspects of it were discussed in the emerging flux model (Heyvaerts *et al.* 1977) and its refinements (Tur & Priest 1976, 1978; Milne & Priest 1981).

The overall picture for a large solar flare (figure 10) is that during the *preflare phase* an active-region prominence and its overlying arcade rises slowly due to some kind of weak eruptive instability or nonequilibrium. At the flare *onset* the field lines that have been stretched out start to break and reconnect, which releases energy impulsively and causes the prominence suddenly to erupt much more rapidly. During the *main phase* reconnection continues and creates hot X-ray loops and Hα ribbons at their footpoints as the field continues to close down. The increase in altitude of the reconnection point causes the locations of the hot loops to rise and of the chromospheric ribbons to move apart. Thus the role of reconnection in large flares is to release the magnetic energy, both in the impulsive and main phase, and sometimes to trigger this release (as in the emerging flux model).

The main questions that MHD addresses are the cause of the eruption and the details of the energy conversion process. Numerical experiments have focused on two problems: first, the details of the closure process, whereby the stretched-out field lines reconnect and close back down; secondly, the global eruption in response to footpoint motions. We summarize some of the work on these in turn below.

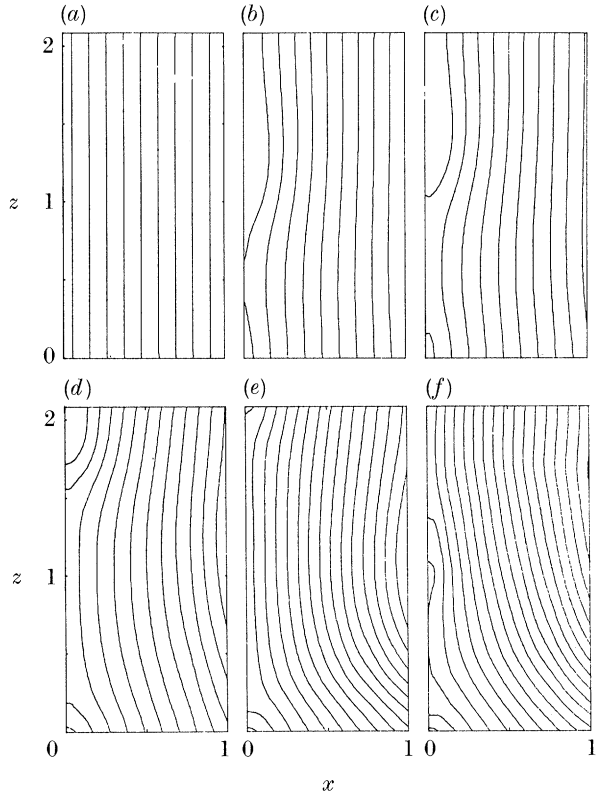

Figure 11. Numerical experiment on the close-down of field lines (Forbes & Priest 1984). $t = 0$ (*a*), 78.22 (*b*), 84.06 (*c*), 99.19 (*d*), 106.19 (*e*), 118.82 (*f*).

(*a*) *The closure process*

Kopp & Pneuman (1976) first suggested that the reconnection process can create flare loops in a two-ribbon flare, with the loops rising and the ribbons separating as the reconnection point rises. Then Cargill & Priest (1982) showed that the magnetic shocks that propagate from the reconnection site can heat the plasma to the observed temperatures of sometimes 10^7 K. Subsequently, the plasma cools and falls to give the classical Hα loops with plasma draining down both legs.

Detailed modelling of the positions of the loops has been undertaken by Poletto & Kopp (1986, 1988) and a kinematic analysis to deduce the resulting electric fields was presented by Forbes & Priest (1982*a*, *b*).

Forbes & Priest (1982*a*, *b*, 1984) set up a numerical experiment with initially vertical field lines in stretched-out equilibrium and anchored at their lower ends to the base of the numerical box due to photospheric line-tying. The experiment showed how the field lines begin to reconnect by the tearing-mode instability and then close down, creating closed loops in a quasi-steady manner (figure 11). The current density contours (figure 12*a*) reveal the location of the diffusion region, and the slow-mode shock waves.

The basic picture of the closure process has recently been refined considerably (figure 12*b*), and recent developments of the numerical experiment have revealed new features of relevance to the observations (Forbes *et al.* 1989) as follows.

1. The quasi-steady reconnection may be modulated in a time-dependent manner

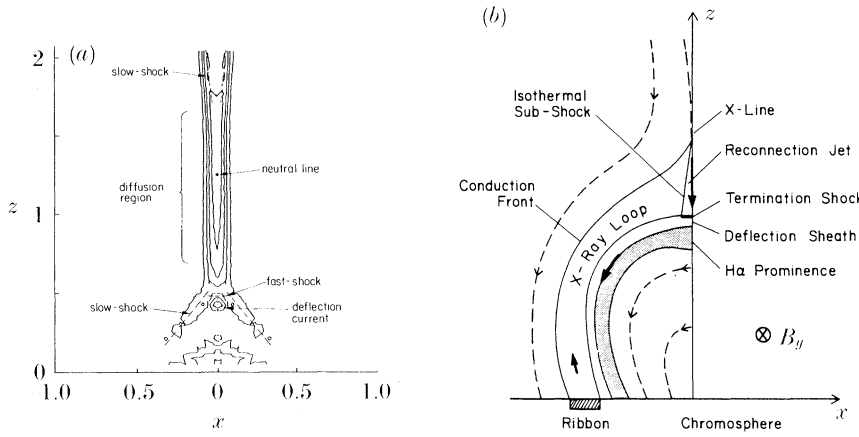

Figure 12 (*a*) Current density contours in numerical experiment on close-down (Forbes & Priest 1984) at $t = 93.38$. (*b*) Schematic of creation of flare loops and Hα ribbons.

as the reconnection enters an impulsive bursty régime (Priest 1986) in which the central diffusion region is so long that it tears (Forbes & Priest 1987), with neutral point pairs being slowly created and then rapidly annihilated. This process is observed in several other numerical experiments (Birn 1980; Biskamp 1982; Lee & Fu 1985; Scholer 1989) and may explain the sudden jumps in loop height that are observed, and the impulsive nature of hard X-ray emission.

2. A fast-mode shock stands in the flow below the reconnection region and slows down the supermagnetosonic stream of plasma as it encounters the obstacle of closed field lines below it (figure 12). At the same time it compresses the plasma. The increase in density drastically reduces the radiative timescale and triggers a thermal condensation which creates cool Hα loops below the hot X-ray loops.

3. A reversed deflection current deflects the flow around the stagnation region.

4. The slow-mode shock wave in the presence of thermal conduction splits up into a conduction front (which propagates down to the chromosphere and across which the temperature rises), together with an isothermal shock wave (across which the density increases).

5. Evaporation is driven from the chromosphere, both by the conduction front and by high-energy particles which travel from the reconnection site along the separatrix ahead of the conduction front. This greatly enhances the density in the hot X-ray loop, in agreement with observations.

6. When the magnetic field is smaller than 10^{-3} T and the field component out of the plane is large enough, a different régime of reconnection is found with submagnetosonic streams of plasma ejected down from the reconnection region. The result is that no fast-shock or rapid condensation is created. Such a régime is appropriate to the eruption of quiescent prominences outside active regions.

(*b*) *The global eruption*

Mikic *et al.* (1988) have modelled the global eruption of a coronal arcade numerically. They have a periodic set of arcades and impose a shearing motion of amplitude $0.01\,v_A$ at the base. With 100×256 mesh points their magnetic Reynolds number is 10^4. The arcade evolves through a series of equilibria, and then at some point reconnects and forms a plasmoid which is ejected out of the top of the numerical box (figure 13). However, there are problems with this experiment, since

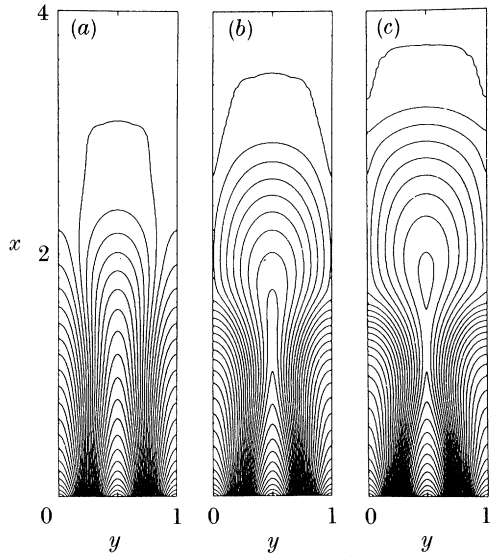

Figure 13. Numerical experiment on global eruption (Mikic *et al.* 1988). $t = 300\ \tau_A$ (*a*), $330\ \tau_A$ (*b*), $340\ \tau_A$ (*c*).

reconnection starts at the edges of the arcade, where it interacts with neighbouring arcades. Also, Biskamp & Welter (1989) find that a single arcade remains stable as it is sheared.

So why does the eruption occur? One possibility is that it results from the interaction of two separate regions, as in the emerging flux model (Heyvaerts *et al.* 1977) and as Mikic *et al.* (1988) and Biskamp & Welter (1989) model numerically. This certainly appears to be the case in some, but not all, flares. So is it possible to understand eruption from a single region?

During the 1980s we considered the linear MHD stability of coronal structures and showed that it is photospheric line-tying which provides the stability and enables the field to store magnetic energy in excess of potential as it is sheared by footpoint motions. When a single flux tube is twisted too much it becomes unstable (Hood & Priest 1979; Einaudi & van Hoven 1983). A simple force-free arcade, at least a linear one, is always stable (Hood & Priest 1990; De Bruyne & Hood 1989). But, when a magnetic island is present in an arcade, which may support a prominence, it can become unstable if the height of the prominence or its length exceed critical values (Hood & Priest 1980). This is consistent with the observation that parts of polarity-inversion lines where the shear is the greatest are the locations of flares (Hagyard *et al.* 1985).

However, a linear instability result has the limitation of saying nothing about the nonlinear development, and so recently we have been considering the possibility of magnetic non-equilibrium or catastrophe. An analysis by Demoulin & Priest (1988) models a prominence as a sheet of mass and current supported in a linear force-free two-dimensional field with field components

$$(B_x, B_y, B_z) = (B_x(A), \partial A/\partial z, -\partial A/\partial y), \tag{6.1}$$

where the flux function A is given by

$$\nabla^2 A + \alpha^2 A = \delta(y)\,\delta(z-h) \tag{6.2}$$

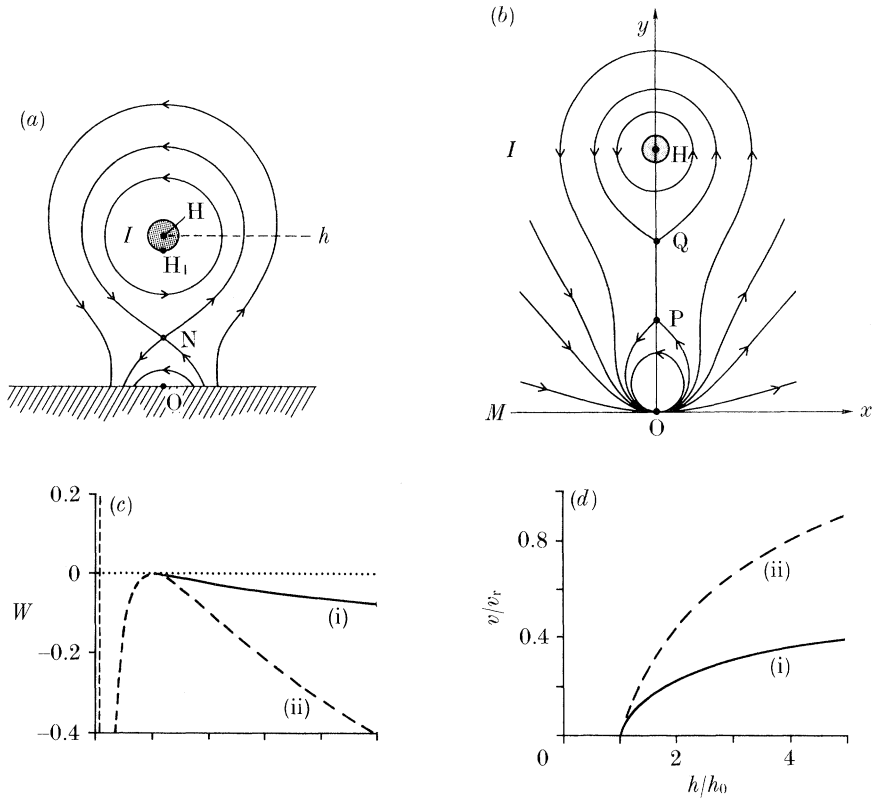

Figure 14 (*a*) The equilibrium magnetic structure in a plane perpendicular to the prominence axis. (*b*) The structure during the eruption with current sheet below the prominence. (*c*) The magnetic work as a function of a filament height h and (*d*) the filament speed as a function of height for (i) no reconnection and (ii) uninhibited reconnection (Priest & Forbes 1990).

when the prominence is located at height $z = h$ above the photospheric surface ($z = 0$). The solution of this may be written as the sum of a complementary function and a particular integral (a Green's function) and the normal field component B_z is imposed at the photosphere. The condition for prominence equilibrium

$$IB_y = mg \tag{6.3}$$

at the prominence of mass m then determines the way the prominence current (I) varies with its height (h). The startling feature is that when the prominence reaches a critical height there is a catastrophe with no neighbouring equilibrium and it erupts. The eruption also occurs if the force-free arcade is sheared too much, in agreement with observations. However, this is only the case when there is a substantial quadrupolar component to the active region: in other words, one needs complexity in the photospheric field, as indeed the observations show.

A similar analysis with a slightly different external field has been carried out by Priest & Forbes (1990). They set up a model for equilibrium and eruption by regarding the prominence as an electric current filament situated at height h in a background active-region field modelled by a magnetic line dipole situated below the photosphere (figure 14*a*). The model is an extension of previous work by Van Tend & Kuperus (1978) and Kuin & Martens (1986). As the filament current or twist

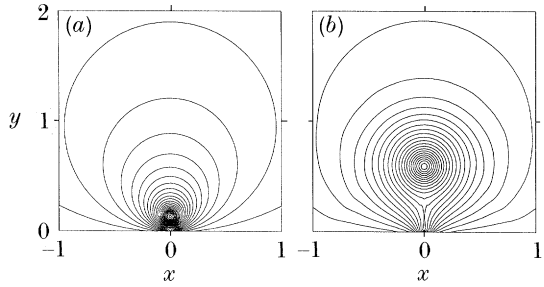

Figure 15. Magnetic field lines for a numerical experiment on the eruption process (Forbes 1991). (*a*) $t = 0$, (*b*) $t = 0.61$.

increases so the prominence rises slowly through a series of equilibria. But when a critical twist or current is exceeded there is no neighbouring equilibrium and a magnetic non-equilibrium or catastrophe takes place, with the unbalanced forces causing the prominence to erupt. The velocity ($\mathrm{d}h/\mathrm{d}t$) of the prominence as a function of time or height may be obtained by solving its equation of motion

$$m\,\mathrm{d}^2h/\mathrm{d}t^2 = IB^*, \tag{6.4}$$

where m is the prominence mass, I its current and B^* the field at the prominence due to the background field.

When the plasma velocity is sub-Alfvenic the magnetic field (B_x, B_y) around the prominence during the eruption may be represented in terms of the complex variable $Z = x + \mathrm{i}y$, where the y axis is vertically upwards (figure 14*b*) as

$$B_y + \mathrm{i}B_x = \mathrm{i}mh^2[(Z^2+p^2)(Z^2+q^2)]^{\frac{1}{2}}/pqZ^2(Z^2+h^2). \tag{6.5}$$

This possesses a line current at $Z = \mathrm{i}h$ (the prominence), a line dipole at $Z = 0$ (the background field) and a cut in the complex plane from $Z = \mathrm{i}p$ to $Z = \mathrm{i}q$ (the prominence current sheet).

When no reconnection is allowed one finds that beyond the non-equilibrium point the magnetic energy declines and the filament speed increases with height (figure 14*c*, *d*). Thus the prominence erupts even if no reconnection is allowed. When reconnection is allowed, however, it is then driven by the eruption. The magnetic work declines more rapidly and the prominence erupts faster, with an energy release eight times faster. The resulting large electric field in the reconnection region may well be important for accelerating fast particles.

Forbes (1991) has been using an FCT code with 50×100 gridpoints to study this process numerically. The initial state and the field lines during the eruption are shown in figure 15, where the creation of the reconnecting current sheet below the erupting prominence can clearly be seen. In a streamline picture a pair of vortices is found below and to either side of the prominence, and plots of density and current density contours reveal the presence of a fast-mode shock travelling ahead of the prominence together with slow-mode shocks near the reconnection site.

7. Conclusion

As we have seen, there have been many developments in the basic theory for reconnection during the past few years. A combination of numerical experimentation and analytical theory has greatly increased our understanding of the effects of boundary conditions in producing a wide variety of different régimes. The field lines

PHILOSOPHICAL TRANSACTIONS OF THE ROYAL SOCIETY A MATHEMATICAL, PHYSICAL & ENGINEERING SCIENCES

in the inflow may be either slightly or greatly curved, and the nature of the inflow may be a fast-mode compression (when the flow is strongly converging) or a slow-mode expansion (when it is strongly diverging). Also the presence of separatrix jets and reversed current spikes has modified the basic models. Furthermore, a consideration of three-dimensional aspects is demanding a rethinking of our basic definitions of reconnection and has shown a new process of magnetic flipping as a means of reconnection without null points.

Numerical experiments of reconnection in a two-ribbon flare have refined and developed the basic picture of fieldline closure that creates flare loops and have explained many observational features. Also, the eruption of a prominence at the start of such a flare may well be caused by a process of magnetic non-equilibrium when the length or height of the prominence is too great.

In future, many developments are expected from more sophisticated numerical experiments and from studies of the three-dimensional aspects. Also, one hopes that the microscopic plasma physicists can make use of the MHD studies, so that further progress can be made on the microscopic processes such as particle acceleration, and so that together we may understand this beautiful phenomenon.

References

Birn, J. 1980 Computer studies of dynamic evolution of the geomagnetic tail. *J. Geophys. Res.* **85**, 1214.

Biskamp, D. 1982 Resistive MHD processes. *Physica Scr.* T**212**, 405–409.

Biskamp, D. & Welter, H. 1989 *Solar Phys.* **120**, 49–77.

Canfield, R. C., de La Beaujardiere, J. & Leka, K. D. 1991 *Phil. Trans. R. Soc. Lond.* A **336**, 381–388. (This volume.)

Cargill, P. & Priest, E. R. 1982 Slow shock heating and the Kopp–Pneuman model for post-flare loops. *Solar Phys.* **76**, 357–375.

De Bruyne, P. & Hood, A. W. 1989 Bounds on ideal MHD stability of line-tied 2D coronal magnetic fields. *Solar Phys.* **123**, 241–269.

Demoulin, P. & Priest, E. R. 1988 Instability of a prominence supported in a linear force-free field. *Astron. Astrophys.* **206**, 336–347.

Einaudi, G. & Van Hoven, G. 1983 The stability of coronal loops: finite-length and pressure-profile limits. *Solar Phys.* **88**, 163–178.

Forbes, T. G. 1990 The role of magnetic reconnection in flares and prominence eruptions. In *Basic plasma processes on the Sun* (ed. E. R. Priest & V. Krishan), pp. 293–302. Dordrecht: Kluwer.

Forbes, T. G. & Priest, E. R. 1982*a* A numerical study of line-tied magnetic reconnection. *Solar Phys.* **81**, 303–324.

Forbes, T. G. & Priest, E. R. 1982*b* Neutral line motion due to reconnection in two-ribbon solar flares and magnetospheric substorms. *Planet. Space Sci.* **30**, 1183–1197.

Forbes, T. G. & Priest, E. R. 1984 Numerical simulation of reconnection in an emerging flux region. *Solar Phys.* **94**, 315–340.

Forbes, T. G. & Priest, E. R. 1987 A comparison of analytical and numerical models of steadily driven reconnection. *Rev. Geophys.* **25**, 1583–1607.

Forbes, T. G., Malherbe, J. M. & Priest, E. R. 1989 The formation of flare loops by magnetic reconnection and chromospheric ablation. *Solar Phys.* **120**, 285–308.

Gratton, F., Heyn, F., Biernat, H., Rijnbeek, R. & Gnavi, G. 1988 MHD stagnation point flows in the presence of resistivity and viscosity. *J. Geophys. Res.* **93**, 7318–7324.

Hagyard, M. *et al.* 1985 Preflare magnetic and velocity fields. In *Energetic phenomena on the Sun* (ed. M. Kundu & B. Woodgate). NASA publication 20-76.

Hesse, M. & Schindler, K. 1988 A theoretical foundation of general magnetic reconnection. *J. Geophys. Res.* **93**, 5559–5567.

PHILOSOPHICAL TRANSACTIONS OF THE ROYAL SOCIETY A MATHEMATICAL, PHYSICAL & ENGINEERING SCIENCES

Heyvaerts, J., Priest, E. R. & Rust, D. M. 1977 An emerging flux model for the solar flare phenomenon. *Astrophys. J.* **216**, 123–137.

Hood, A. W. & Priest, E. R. 1979 Kink instability of solar coronal loops as the cause of small flares. *Solar Phys.* **64**, 303–321.

Hood, A. W. & Priest, E. R. 1980 Magnetic instability of coronal arcades as the origin of two-ribbon solar flares. *Solar Phys.* **66**, 113–134.

Jardine, M. & Priest, E. R. 1988 Weakly nonlinear theory of fast steady-state magnetic reconnection. *J. Plasma Phys.* **40**, 143–161.

Jardine, M., Allen, H. R., Grundy, R. E. G. & Priest, E. R. 1991 A family of 2D nonlinear-solutions for magnetic field annihilation. (Submitted.)

Kopp, R. A. & Pneuman, G. W. 1976 Gas–magnetic field interactions in the solar corona. *Solar Phys.* **18**, 258–270.

Kuin, N. & Martens, P. 1986 A dynamic model of filament eruptions and two-ribbon flares. In *Coronal and prominence plasmas* (ed. A. Poland) pp. 241–245. NASA CP 2442.

Lau, Y.-T. & Finn, J. M. 1930 3D kinematic reconnection in the presence of field nulls and closed field lines. *Astrophys. J.* **350**, 672–691.

Lee, L. C. & Fu, Z. F. 1985 A theory of magnetic flux transfer at the Earth's magnetosphere. *Geophys. Res. Lett.* **12**, 105.

Mikic, Z., Barnes, D. C. & Schnack, D. D. 1988 Dynamic evolution of a solar coronal magnetic field arcade. *Astrophys. J.* **328**, 830–847.

Milne, A. M. & Priest, E. R. 1981 Internal structure of reconnecting current sheets and the emerging flux model for solar flares. *Solar Phys.* **73**, 157–181.

Parker, E. N. 1963 The solar flare phenomenon and the theory of reconnection and annihilation of magnetic fields. *Astrophys. J. Supp.* **8**, 177–211.

Petschek, H. E. 1964 Magnetic field annihilation. In *AAS–NASA Symposium on physics of solar flares*, pp. 425–439. NASA SP-50.

Poletto, G. & Kopp, R. A. 1986 Macroscopic electric fields during two-ribbon flares. In *The lower atmosphere of solar flares* (ed. D. Neidig) pp. 453–465. Sacramento Peak.

Poletto, G. & Kopp, R. A. 1988 The magnetic geometry and structure of the giant post-flare arch of 21–22 May, 1980. *Solar Phys.* **116**, 163–178.

Priest, E. R. 1982 *Solar MHD*. Holland: Reidel.

Priest, E. R. 1986 MHD theories of solar flares. *Solar Phys.* **104**, 1–18.

Priest, E. R. 1987 Appearance and disappearance of magnetic flux at the solar surface. In *The role of fine-scale magnetic fields on the structure of the solar atmosphere* (ed. E. Schroter, M. Vazquez & A. Wyller) pp. 297–316. Cambridge University Press.

Priest, E. R. & Forbes, T. G. 1986 New models for fast steady-state reconnection. *J. Geophys. Res.* **91**, 5579–5588.

Priest, E. R. & Forbes, T. G. 1989 Steady reconnection in three dimensions. *Solar Phys.* **119**, 211–214.

Priest, E. R. & Forbes, T. G. 1990 Magnetic field evolution during prominence eruptions and two-ribbon flares. *Solar Phys.* **126**, 319–350.

Priest, E. R. & Forbes, T. G. 1991 Magnetic flipping – reconnection in three dimensions without null points. (Submitted.)

Priest, E. R. & Lee, L. C. 1990 Nonlinear magnetic reconnection models with separatrix jets. *J. Plasma Phys.* **44**, 337–360.

Schindler, K., Hesse, M. & Birn, J. 1988 General magnetic reconnection, parallel electric fields and helicity. *J. Geophys. Res.* **93**, 5547–5558.

Scholer, M. 1989 Undriven reconnection in an isolated current sheet. *J. Geophys. Res.* **94**, 8805–8812.

Sonnerup, B. U. O. 1970 Magnetic field reconnection in a highly conducting incompressible fluid. *J. Plasma Phys.* **4**, 161–174.

Sonnerup, B. U. O. 1988 On the theory of steady state reconnection. *Comp. Phys. Comm.* **49**, 143.

PHILOSOPHICAL TRANSACTIONS OF THE ROYAL SOCIETY A MATHEMATICAL, PHYSICAL & ENGINEERING SCIENCES

Sonnerup, B. U. O. & Priest, E. R. 1975 Resistive MHD stagnation point flows at a current sheet. *J. Plasma Phys.* **14**, 283–294.

Sweet, P. A. 1958 The neutral point theory of solar flares. *IAU Symp.* **6**, 123–134.

Tur, T. & Priest, E. R. 1976 The formation of current sheets during the emergence of new magnetic flux from below the photosphere. *Solar Phys.* **48**, 89–100.

Tur, T. J. & Priest, E. R. 1978 A trigger mechanism for the emerging flux model of solar flares. *Solar Phys.* **58**, 181–200.

Van Tend, W. & Kuperus, M. 1978 The development of coronal electric current systems in active regions and their relation to filaments and flares. *Solar Phys.* **59**, 115–128.

Vasyliunas, V. 1975 Theoretical models of magnetic field line merging. *Rev. Geophys. Space Phys.* **13**, 303–336.

Discussion

K. J. H. Phillips (*Rutherford Appleton Laboratory, U.K.*). The observations of Hα loop prominences show that the height of successive prominences increases in a particular way (in fact proportional to $t^{\frac{1}{2}}$, where t is time after flare) with time. Do your numerical simulations predict such a relation?

E. R. Priest. The models are in qualitative agreement with the observed rate of rise of flare loops. Also Forbes & Priest (1982*a*, *b* and *J. Geophys. Res.* **88**, 863–870 (1983)) compared a kinematic model of loop rise with the observations and showed that the observed decrease in the rate of rise could be produced by a constant rate of reconnection. However, to make a detailed quantitative comparison, one needs an accurate measure of the coronal magnetic field strength.

M. G. Haines (*Imperial College, London, U.K.*). Is a realistic value of the Lundquist number being used in your modelling of reconnection?

E. R. Priest. The Lundquist number used in the numerical experiments is at most 10^3, which of course is much smaller than the classical value in a flare of 10^{10} or 10^{12}. There is no way in the foreseeable future that such values could be employed in a numerical experiment. Instead, the philosophy of numerical experimentation is to adopt as large a value as possible and to deduce basic features of the physical processes and scaling laws which can be extrapolated to realistic Lundquist numbers. Furthermore, in a flare the Lundquist numbers are in reality probably far smaller than the classical values due to the presence of turbulence: indeed Forbes & Priest (*Solar terrestrial physics: present and future* (ed. D. Butler & K. Papadopoulos), pp. 1–35. NASA RP 1120 (1984)) worked backwards and used the observed loop motion to deduce a turbulent Lundquist number of 10^8.

PHILOSOPHICAL TRANSACTIONS OF THE ROYAL SOCIETY A MATHEMATICAL, PHYSICAL & ENGINEERING SCIENCES